Quantifying Creep Damage in a Metallic Alloy Using Acousto-Ultrasonics

Andrew L. Gyekenyesi, Harold E. Kautz, and Robert E. Shannon

(Submitted 13 December 2001)

Due to elevated temperatures and excessive stresses, turbine components may experience creep behavior. As a result, it is desirable to monitor and assess the current condition of such components. This study used the acousto-ultrasonics (AU) method in an effort to monitor the state of the material at various percentages of expended (i.e., used-up creep life) creep life in the nickel base alloy, Udimet 520. A stepped specimen (i.e., varying cross-sectional area) was used, which allowed for a post mortem nondestructive evaluation (NDE) analysis of the various levels of expended life. The overall objectives in this study were two-fold: First, a user-friendly, graphical interface AU system was developed, and second, the new AU system was applied as a NDE tool to assess distributed damage resulting from creep. The experimental results demonstrated that the AU method was able to detect material changes as a function of expended creep life.

Keywords acousto-ultrasonics, creep damage, health monitoring, metallic alloy, nondestructive evaluation, turbine

1. Introduction

In recent years emphasis has been placed on the early detection of material changes experienced in turbine power plant components. During the scheduled overhaul of a turbine, the current techniques of examination of various hot-section components aim to find flaws such as cracks, wear and erosion, as well as excessive deformations. Thus far, these localized damage modes have been detected with satisfactory results.[1] However, the techniques used to find these flaws provide no information on life until the flaws are actually detected. Major improvements in damage assessment, safety, as well as more accurate life prediction could be achieved if nondestructive evaluation (NDE) techniques could be used to sense material changes that occur prior to the localized defects mentioned above.

As a result of elevated temperatures and applied stresses, turbine components are subject to creep processes that limit the components' life. For polycrystalline metals, the permanent deformations associated with creep are due to various stress-assisted, thermally activated micromechanisms. These include the generation and mobilization of dislocations, escape of dislocations from their glide planes, grain boundary sliding and diffusion of atoms, and point defects.[2] These mechanisms characterize the majority of the creep life as defined by the primary and secondary portions of a typical strain vs time creep curve. As failure approaches, an increase in strain rate is noticed and is identified as the tertiary portion of the creep curve. The increase in the strain rate is assumed to occur as a result of additional mechanisms such as the growth and accumulation of cavities along grain boundaries. The growing cavities reduce the effective area of the material with the final result being creep rupture. (For a full discussion of creep behavior, the reader is advised to consult the textbook by Shames and Cozzorelli[2] as well as the textbook by Gittus.[3]

The goal of this study was to use a NDE technique that discloses distributed material changes that occur prior to the localized damage detected by the current methods of inspection. The creep processes were the life-limiting condition of interest and the NDE technique used was acousto-ultrasonics (AU). AU is a NDE technique that utilizes two ultrasonic transducers to interrogate the condition of a test specimen. The sending transducer introduces an ultrasonic pulse at a point on the surface of the specimen whereas a receiving transducer detects the signal after it has passed through the material. The aim of the method is to correlate certain parameters of the detected waveform to characteristics of the material between the two transducers. Here, the waveform parameter of interest is the attenuation due to internal damping for which information is being garnered from the frequency domain. The parameters used to indirectly quantify the attenuation are the ultrasonic decay rate as well as various moments of the frequency power spectrum.[4-6] To attain the objective of a NDE technique that can monitor distributed damage due to creep, a new, user-friendly, graphical interface, AU system was developed at NASA Glenn Research Center. The AU system is a multifunction system that captures and digitizes the signal from the receiving ultrasonic transducer and then conducts post-test signal analysis. The system's post processing software calculates multiple parameters utilized to study the material of interest.

Creep tests were conducted on the nickel base alloy, Udimet 520. AU measurements were performed at various percentages of expended life. Rather than periodically interrupting the creep tests to obtain AU data, a stepped specimen (i.e., a varying cross-sectional gage area) was used. This specimen design allowed the creep tests to continue, uninterrupted, until creep rupture occurred. The failure occurred in the smallest cross-sectional area. Each specimen had four different cross-sectional areas within the gage section, each of which corre-

Andrew L. Gyekenyesi, OAI/Glenn Research Center, Cleveland, OH 44135; **Harold E. Kautz,** NASA Glenn Research Center, Cleveland, OH 44135; and **Robert E. Shannon,** Siemens Westinghouse Power Company, Science and Technology Center, Pittsburgh, PA 15235. Contact e-mail: andrew.l.gyekenyesi@grc.nasa.gov.

Table 1 Creep Specimen Test Matrix (*) and Results at 732 °C

Predicted Life, h (*)	100	200	400	800
Stress: 100% expanded life, MPa	522	483	447	413
Stress 50% expanded life, MPa	483	447	413	382
Stress: 25% expanded life, MPa	447	413	382	354
Stress: 12.5% expanded life, MPa	413	382	354	327
Creep failure time, h (†)	260	321	745	1395
Failure strain, % (†)	5.6	5.3	9.1	8.6
Specimen ID	A1	C1	B1	B2

(*) Predicted time to creep failure for smallest area gage section and stresses for the multiple gage widths were based on the conventional creep data of reference 6.
(†) Creep failure time and failure strain are actual results for the 100% expanded creep life gage sections of the specimens tested here.

Table 2 Creep Specimen Test Matrix (*) and Results at 816 °C

Predicted Life, h (*)	100	200	400	800
Stress: 100% expanded life, MPa	419	374	334	330
Stress: 50% expanded life, MPa	387	346	310	305
Stress: 25% expanded life, MPa	359	321	286	282
Stress: 12.5% expanded life, MPa	332	296	265	261
Creep failure time, h (†)	23	56	144	705
Failure strain, % (†)	9.6	5.6	10.9	11.0
Specimen ID	C2	D1	D2	A2

(*) Predicted time to creep failure for smallest area gage section and stresses for the multiple gage widths were based on the conventional creep data of reference 6.
(†) Creep failure time and failure strain are actual results for the 100% expended creep life gage sections of the specimens tested here.

sponded to a different level of expended life. The following section describes the specimen design, the AU system, as well as the experimental procedure.

Lastly, it should be noted that the vast majority of research concerning the AU technique has been based on characterizing damage in composite materials (e.g., polymer matrix composites, ceramic matrix composites, etc.). For the most part, the distributed damage in composites is in the form of fiber-matrix debonding (interface failure), matrix cracking that can be intralaminar or interlaminar (delaminations), and fiber fracture or fiber micro-buckling.[7] These types of damage mechanisms are known to be highly attenuating. It is much more challenging to gauge the microstructural evolution that occurs in monolithic metallic alloys during creep. The change in attenuation resulting from distributed damage in metals is significantly lower than that seen in most composites.

2. Experimental Methods

The material used for this study was Udimet 520, a nickel base alloy. Creep specimens were designed with a multi-step gage region to provide areas of different remaining life (see Fig. 2 in the Results section for a photograph of a fractured specimen). The overall length of the specimens was 15 cm (6 in); each step as well as the grip sections had a length of 2.5 cm (1 in). The thickness was 0.4 cm (0.16 in). The four-gage widths ranged from 2.25 to 3.0 cm (0.9 to 1.2 in) and were designed to correspond to 12.5, 25, 50, and 100% expended life with fracture occurring in the cross-section of smallest area. Note that life was defined as time to complete fracture for a given fixed load. The applied loads for each specimen were selected by reviewing conventional creep data for this particular material.[8] Specimens were stressed at various levels at 732 °C (1350 °F) and at 816 °C (1500 °F). Tables 1 and 2 summarize the test matrix as well as the results. A total of eight specimens were provided for the AU analysis; four specimens that were creep tested at 732 °C (1350 °F) and four specimens that were creep tested at 816 °C (1500 °F). Lastly, it should be noted that the goal was to provide creep-tested specimens with various levels of expended life for NDE analysis using the new AU system. This particular material has been fully characterized previously.[8] Therefore, in-depth details of the material behavior are not discussed here.

As stated earlier, the fundamental aspect of the AU method entails introducing a mechanical excitation at one point on a material surface and sensing the resulting disturbance at another spot on the material surface.[9-11] Figure 1 displays a general diagram of the AU experimental set-up used for this study. The method of excitation involved the utilization of piezoelectric transducers. A pulsing transducer was used to introduce a high-frequency, broadband ultrasonic pulse into the specimen. The ultrasonic pulse was allowed to distribute itself diffusely into the specimen. The term diffuse relates to an incoherent ultrasonic wave that has lost all phase information. A diffuse wave is a complicated superposition of wave modes and sample reverberations that resembles an acoustic emission signal. This is somewhat different than traditional ultrasonics, in which a well-defined acoustic pulse is monitored. The decay of this resulting incoherent field is then examined as a function of frequency.[5,6]

Typically in AU, two separate transducers are applied at some fixed separation on the face of the specimen. An ultrasonic wave is introduced and allowed to propagate along the length of the specimen. The fact that the characterization can be directed along the primary load direction in structures indicates an important advantage of this technique over typical ultrasonic techniques (e.g., C-scan). Because the sub-areas (defining the various levels of expended life; see above) of the creep specimens were relatively small with respect to the size of a typical transducer, a dual element transducer was used (see Fig. 1). The dual element transducer had a single-body construction that contained two independent piezoelectric elements separated by an acoustic shield. Hence, one piezoelectric element acted as the pulser and the other acted as the receiver. The 2.25 MHz broadband, dual-element transducer used for this study had a 6 mm (0.25 inch) diameter contact area and was manually joined to the specimen using a gel couplant. The shape of the contact area for each individual piezoelectric element within the single transducer body was a half-circle. Furthermore, the transducer was aligned perpendicular to the face of the specimen (see Fig. 1). The computer's data acquisition rate was set to 50 MHz, and the acquisition time window was 10 μs (496 data points). The experimental variables were selected

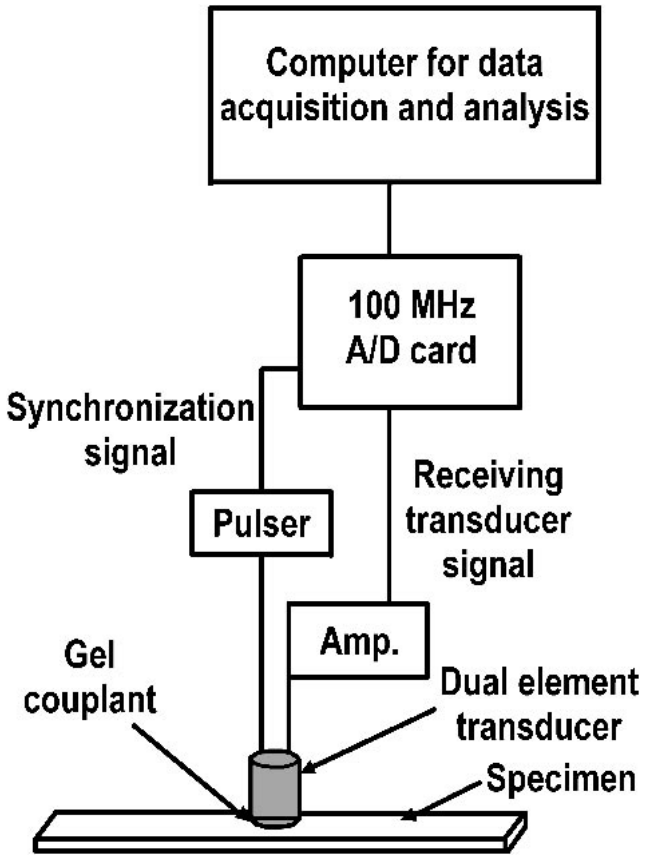

Fig. 1 Schematic of AU set-up

after numerous trials that were conducted for optimizing the received signal. By observing the received signals during the trials, one can adjust and optimize certain parameters such as the transducer frequency, signal amplitude, and time duration. One optimization condition was concerned with selecting a high enough frequency so as to localize the ultrasonic signal to the specimen position of interest. When conducting the tests, the piezoelectric elements were aligned to produce an ultrasonic wave path in the length direction of the specimen. The results included four measurements for any given longitudinal position on the specimen. The four conditions of the measurements involved studying each face of the specimen as well as rotating the transducer 180 degrees. For each creep specimen, 18 positions were analyzed along the centerline in the length direction. Next, a discussion relating to the methods of post-test signal analysis is presented.

Two main approaches for analyzing the received diffuse signal are used in the newly developed AU system. First to be discussed is the analysis method that is used at NASA GRC.[4,6,12] Titled the diffuse field decay rate, the method involves quantifying the internal damping of vibrational energy in materials. The analysis is based on the premise that a diffuse ultrasonic field in an isolated sample will decay only from internal absorption mechanisms and that contributions of damping by air, transducers, and fixturing are minimal. Damping is measured through determination of the volume averaged decay rate of the ultrasonic field as a function of frequency and time. A greater decay rate indicates a greater amount of internal damping. Determining the decay rate is accomplished by dividing the recorded waveform into a number of time windows (eight windows were used for this study), after which fast Fourier transforms (FFTs) are performed to obtain the power spectrums. Note that the power spectrum is the square of the amplitude function at a given frequency. The total energy of each time window is calculated using the power spectrum (i.e., the area under the power spectrum plot). Further refinement is achieved by obtaining the energy content of various frequency windows within the power spectrums. Lastly, an exponential decay curve is fitted to the plot of energy versus time window. The exponent in the equation is defined as the diffuse field decay rate. Mathematically the equation is expressed as follows:

$$M_0(f_{low}, f_{high}, t) = \alpha(f_{low}, f_{high}) e^{-\beta(f_{low}, f_{high})t} \quad \text{(Eq 1)}$$

where t is time; f_{low} and f_{high} are the low and high frequency filter limits; M_0 is the mean square value of the power spectrum as a function of frequency and time; α is the intercept as a function of frequency (this value is not used in this study); and β is the diffuse field decay rate as a function of frequency.

The second method of post processing involves working with the entire time domain signal and again conducting a FFT to obtain the power spectrum.[12] Certain parameters concerning the power spectrum were shown to be sensitive to various types of damage in composite materials.[5,13] Called the shape parameters, the general equations are defined as follows:

$$S_{r,k} = \frac{M_r}{M_{r-k} f_c^k} \quad \begin{matrix} k = 1,2,3\ldots \\ r = 2,3,4\ldots \\ r > k \end{matrix} \quad \text{(Eq 2)}$$

where

$$M_r = \int_{f_{low}}^{f_{high}} S(f) f^r \, df \quad \text{(Eq 3)}$$

$S(f)$ is the power spectral density, f is the frequency, and f_c is the location of the centroid found by the following expression:

$$f_c = \frac{M_1}{M_0} \quad \text{(Eq 4)}$$

Several of the moments and moment ratios can be given physical interpretations. For example, M_0 is the mean square value of the power spectral density (i.e., the area under the power spectrum). In addition,

$$f_0 = \left(\frac{M_2}{M_0}\right)^{\frac{1}{2}} \quad \text{(Eq 5)}$$

is the frequency of mean crossings with positive slopes and

$$f_p = \left(\frac{M_4}{M_2}\right)^{\frac{1}{2}} \quad \text{(Eq 6)}$$

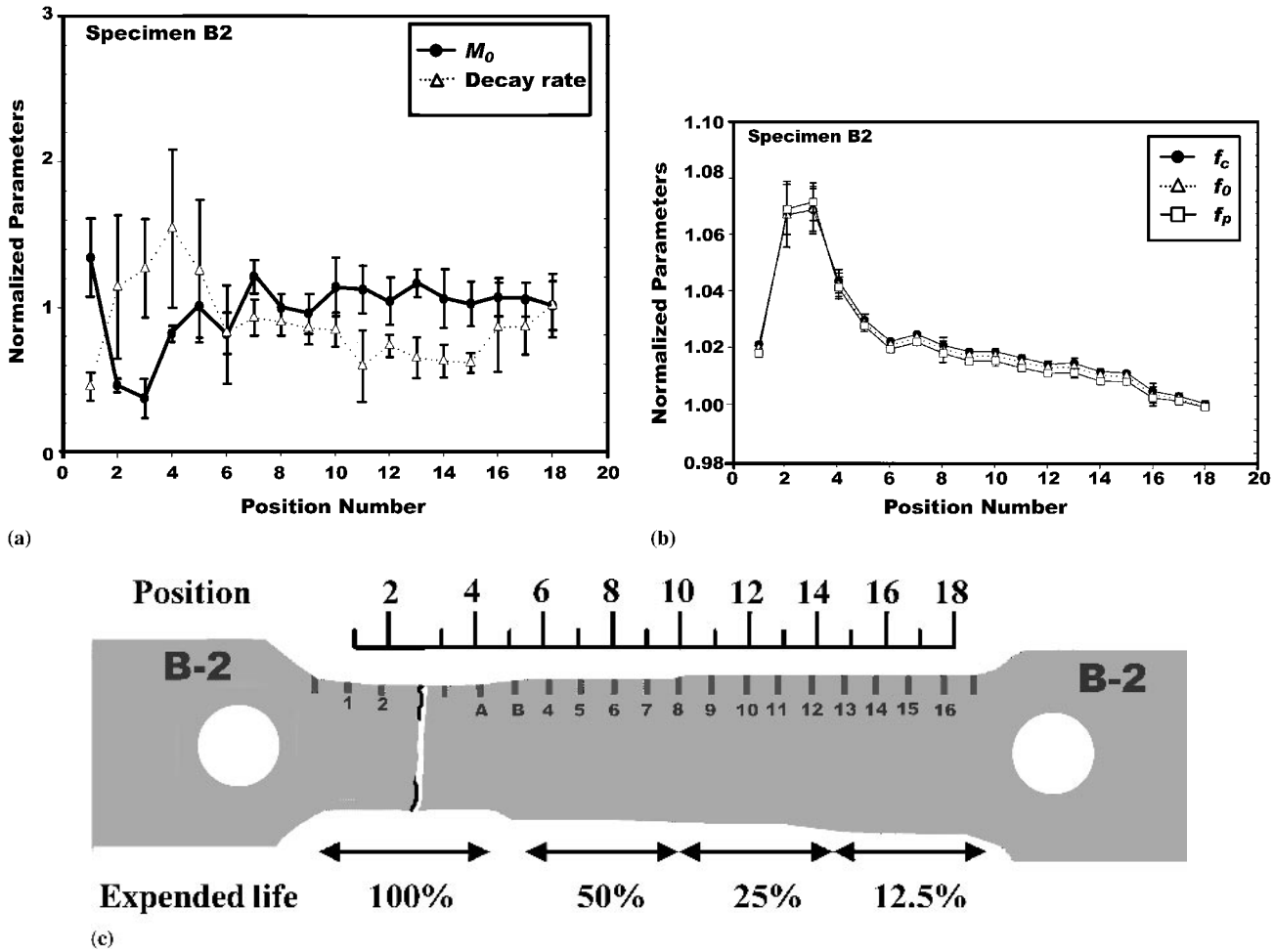

Fig. 2 AU parameters as functions of expended creep life (specimen B2 tested at 732 °C): **(a)** M_0 and decay rate; **(b)** f_c, f_0, and f_p; and **(c)** photograph of fractured specimen. The four gage areas on the specimen represent from left to right, 100, 50, 25, 12.5% expended creep life. (Use scale above the specimen for position location.)

is the frequency of maxima in the time domain. Note that Eq 2 through 6 provide scalar values that capture the general characteristics of the power spectrum function. The diffuse field decay rate as well as M_0, f_c, f_0, and f_p were implemented in the new AU software and were used in this study to assess the creep-tested material.

3. Results

The time to fracture results as a function of stress and temperature are presented in Tables 1 and 2. Each of the creep specimens fractured in the middle of the narrowest gage section, representing 100% expended creep life. Figure 2 displays the AU data for a creep specimen tested at 732 °C (1350 °F). To allow for the simultaneous viewing of the multiple parameters, each AU parameter was normalized by its respective position 18 value. These normalization values were located in the widest gage section of the specimen (i.e., the 12.5% expended life region). The error bars in the plots represent one standard deviation of the four repetitive measurements at each position. In addition, a photo of a creep specimen is displayed adjacent to the plots to indicate the longitudinal position of each of the data points. Positions 1-4, 5-9, 10-14, and 15-18 corresponded to 100, 50, 25, and 12.5% expended creep life, respectively. For this particular specimen, the fracture occurred between positions 2 and 3 in the plots. Figure 2 shows that essentially all the parameters for this particular specimen indicated a functional dependence on position (i.e., expended creep life or damage). These included the diffuse field decay rate, M_0, f_c, f_0, and f_p, although the diffuse field decay rate and M_0 were limited to changes observed near the fracture surface. After experimenting with various frequency-filtering windows, the best results were obtained when applying a frequency window from 1.9 to 2.9 MHz. This window corresponded to the central frequency of the broadband transducer. Hence, the majority of the ultrasonic energy was located within this window, thereby increasing the signal to noise ratio. Although using the frequency window drastically reduced data scatter and strengthened the relationship between the parameters and the expended creep life, it did institute the mathematical loss of identity between f_c, f_0, and f_p. The smaller the frequency window, the

more these parameters behaved alike. Lastly, there appeared to be a skewing of the AU values at the transition regions between each of the gage areas. This is evident by viewing Fig. 2(b) and noting the sloping pattern within each gage area.

The data shown in Fig. 2 indicate that there was an overall increase in attenuation of the ultrasonic signal with accumulated damage (i.e., expended creep life), as expected. This was reflected in the increased diffuse field decay rate as well as the decreased ultrasonic wave energy, M_0. Another effect of the creep damage was the preferential attenuation of the signal's low frequency components. This behavior caused f_c, f_0, and f_p to increase with creep damage. Similar trends were observed for all the AU parameters in each of the eight creep specimens, regardless of the applied stress or temperature.

It is observed in Fig. 2(b) that f_c, f_0, and f_p had the least scatter and highest degree of correlation to expended creep life. Again, this was the case for all the creep specimens. Therefore, to simplify the presentation of the data, from this point forward the results are focused on analyzing f_c, the centroid of the power spectrum. Figure 3 displays f_c as a function of position for each of the eight creep specimens.The specimens with the strongest dependence on expended creep life were C1 and B2 at 732 °C (1350 °F) and C2 at 816 °C (1500 °F). The rest of the specimens captured only the late stage material changes seen in the vicinity of the failure surface. Lastly, specimen B1 appeared to standout in comparison to the other specimens. No explanation can be given at this time on why specimen B1 was an outlier. Concerning specimen B1, it was apparent from the start (i.e., 12% expended life; positions 15-18) that the values for f_c were high compared to the other specimens.

For the eight creep specimens, the average change from the minimum to maximum f_c was 6%. The minimum f_c values were located in the largest gage areas (i.e., the gage areas representing 12.5% expended creep life) whereas the maximum f_c values were adjacent to the fracture surfaces. The average standard deviation of the four repetitions at each location for all eight specimens (144 positions) was 0.25%. The overall change in f_c was 24 times larger than the average standard deviation of the repetitive measurements. This was a good result considering that for each of the four repetitions the transducer was manually removed and reapplied (see Experimental Methods section).

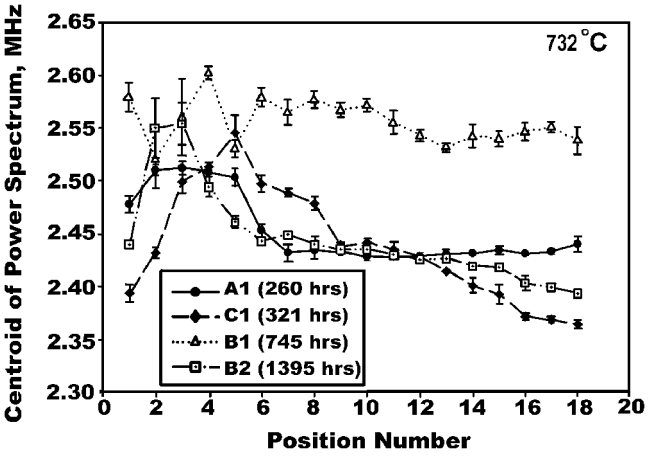

(a)

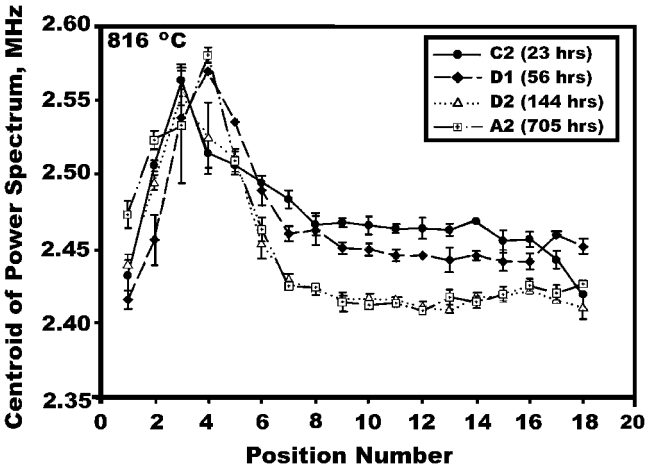

(b)

Fig. 3 Centroid of power spectrum (f_c) as a function of specimen position (see Fig. 2c) for each of the eight creep specimens at **(a)** 732 °C and **(b)** 816 °C. Indicated in the legend is the time to failure for each specimen. Note that all fractures occurred between positions 2 and 5.

4. Discussion and Conclusions

The AU technique seems to show promise as an NDE tool for empirically gauging the level of expended creep life in metallic alloys. To gain further understanding, the AU results need to be correlated to the microstructural changes experienced during creep and thermal aging. At this point, a relatively safe assumption could be made concerning the creep specimens. The AU parameters were probably altered as a result of increasing cavitation or porosity as the 100% creep life was approached. This was most notable when viewing the AU parameters measured at positions close to the fracture surface. Large changes in the measured AU response were seen at these locations.

The AU data indicated the potential for an empirical relationship that can be developed and used as a "before and after" measuring tool after the progression of damage within a single specimen. This recommendation for limiting the AU analysis to single specimens is the result of the specimen-to-specimen variations seen in Fig. 3. These same material variations may have existed within the specimens and contributed to the inconsistencies seen in some of the data. Allowing the ultrasonic pulse to propagate through a larger amount of material may average out some of these material variations. For this study, the length of ultrasonic propagation was limited by the size of the specimen's gage section.

In conclusion, the following achievements were accomplished during this study: A new user- friendly, graphical interface AU system was developed that allowed for the simultaneous calculation of numerous AU parameters. Next, by using a stepped creep specimen design (i.e., varying cross-sectional area), it was shown that the AU technique could be used to monitor creep damage in metallic alloys. It was assumed that the increased cavitation or porosity due to accumulating creep damage-induced changes in the ultrasonic attenu-

ation as depicted by the various AU parameters. After studying the results, the centroid of the power spectrum was found to have the least scatter and the strongest relationship with expended creep life. As noted in the Introduction, the AU technique has been studied extensively as a damage assessment tool for composite materials. Here, in addition to assembling the new AU software package, the AU technique has been expanded to the domain of metallic alloys.

In the future, it is imperative to analyze stepped specimens with additional levels of expended creep life. Such specimens would allow a more definite characterization of the sensitivity of the AU technique. Furthermore, various metallic systems with dissimilar failure mechanisms need to be studied. To achieve added confidence in an empirical AU creep life model, studies need to be conducted which analyze the effects of changing boundary conditions (e.g., effect of static or residual stress, temperature, transducer contact force, etc.).

Acknowledgments

The authors would like to acknowledge Dr. George Y. Baaklini of the NASA Glenn Research Center at Lewis Field as well as the Aviation Safety Program for providing the funding for this study. In addition, the authors thank Dr. Wei Cao of the West Virginia University Institute of Technology for his support concerning the AU system's software programming.

References

1. W. Lempp, N. Kasik, and U. Feller: "Nondestructive Degradation Evaluation of Ferritic Steels for High Temperature Applications," in *Nondestructive Characterization of Materials II*, J.F. Bussiere, J.P. Monchalin, C. O. Ruud, and R.E. Green Jr., ed., Plenum Press, New York, 1987, pp. 441-49.
2. I.H. Shames and F.A. Cozzarelli: *Elastic and Inelastic Stress Aanalysis,* Prentice Hall, Englewood Cliffs, NJ, 1992.
3. J. Gittus: Creep, *Viscoelasticity and Creep Fracture in Solids,* Applied Science Publishers LTD, London, 1975.
4. H.E. Kautz: Determination of Plate Wave Velocities and Diffuse Field Decay Rates with Broadband Acousto-Ultrasonic Signals," *Second International Conference on Acousto-Ultrasonics*, ASNT, Atlanta, GA, 1993.
5. A. Tiwari: "Real Time Acousto-Ultrasonic NDE Technique for Monitoring Damage in Ceramic Composites Under Dynamic Loads," NASA Cr-198374, Aug 1995.
6. R.L.Weaver: "Diffuse Field Decay Rates for Material Characterization," *Solid Mechanics Research for Quantitative Nondestructive Evaluation*, J.D. Achenbach and Y. Rajapaskie, ed., 1987, Martinus Nijhoff, The Netherlands, pp. 425-34.
7. A.L. Gyekenyesi: "Isothermal Fatigue, Damage Accumulation, and Life Prediction of a Woven PMC," NASA Cr-1998-206593, Mar 1998.
8. R. Widmer, J.M. Dhosi, A. Mullendore, and N.J. Grant: "Mechanisms Associated with Long Time Creep Phenomena: Part I. Presentation of Creep Data and Structural Analysis," AFML-TR-65-181 Part 1.
9. A. Vary and K.J. Bowles: "Ultrasonic Evaluation of the Strength of Unidirectional Graphite Polyimide Composites", *Proceedings of the Eleventh Symposium on Nondestructive Testing*, Southwest Research Institute, San Antonio, TX, 1977, pp. 242-58.
10. A. Vary and K.J. Bowles: "Use of Ultrasonic Acoustic Techniques for Nondestructive Evaluation of Fiber composite Strength", *Proceedings of 33rd Annual Conference*, SPI, New York, 1978, Section 24A, pp. 1-5.
11. M.T. Kiernan and J.C. Duke: "A Physical model for the Acousto-Ultrasonic Method," NASA Cr-185294, Oct 1990.
12. L.A. Lott and D.C. Kunerth: "NDE of Fiber-Matrix Interface Bonds and Material Damage in Ceramic/Ceramic Composites," *Conference on Nondestructive Evaluation of Modern Ceramics*, Columbus, OH, July 9-12, 1990, pp. 135-39.
13. R.Talreja, A. Govada, and E.G. Henneke, "Quantitative Assessment of Damage Growth in Graphite Epoxy Laminates by Acousto-Ultrasonic Measurements," *Rev. Prog. Quantitative Nondestructive Eval.* 1984, *3,* pp. 1099-106.